



## SYNTHESIS AND CHARACTERIZATION OF $\text{LiCo}_{1-x}\text{Fe}_x\text{O}_2$

V.GANGADHAR, P.SATEESH,G.S.KUMAR, G.PRASAD\*

Department of Physics, Osmania University, Hyderabad 500 007, India.

\*Corresponding author. Tel:+91 40 27682242: fax: +91 40 27099020 E-mail  
address:gudurup@gmail.com

### ABSTRACT

$\text{LiMO}_2$  are lithium based layered materials (M transition metal ion) one important electrolyte materials for solid state battery applications. High storage energy density, long life time, stability and range of operating temperatures are some of the important parameters that determine the functionality of these materials. In the present paper  $\text{LiCo}_{1-x}\text{Fe}_x\text{O}_2$  material is synthesized and characterized.  $\text{LiCo}_{1-x}\text{Fe}_x\text{O}_2$  compounds with  $x = 0, 0.1, 0.2, 0.3, 0.4, 0.5, 0.6, 0.7, 0.8, 0.9$  and  $1.0$  were synthesized through Sol-Gel method. X-ray diffraction studies and scanning electron microscopic studies were carried out to confirm the phase formation and to observe the surface morphology. A variation of the crystal structure was observed from trigonal (rhombohedral) to cubic with increasing the "Fe" concentration. DC conductivity measurements were done in the temperature region RT-500°C. Impedance spectroscopic studies were done in the frequency region 100Hz to 1MHz in the temperature region RT-500°C. Activation energies of conduction and relaxation were calculated. Increasing of AC conductivity was observed with increasing "Fe" concentration.

**Keywords:** Sol - Gel synthesis, XRD, DC & AC conductivity, Impedance spectroscopy.

### INTRODUCTION

$\text{LiMO}_2$  layer oxide (M=Co,Fe) materials have been intensively studied for the utilization as positive electrode materials in high energy density batteries and widely used in lithium ion rechargeable batteries as electrolyte material. The main advantages of these materials were high energy density, long cycle life, good safety features, stable discharge properties and wide range of operating temperatures [1].  $\text{LiCoO}_2$  is the most widely used material for commercial lithium ion batteries due to its excellent electrochemical cycling stability in rechargeable batteries. The disadvantage like highly toxic, high cost, low practical capacity made this material use in less applications[2].  $\text{LiFeO}_2$  has become an alternative materials due to its most abundance and non-toxicity of iron. To study the effect of the substitution of Fe for Co in the  $\text{LiCoO}_2$ , ceramics prepared with the formula  $\text{LiCo}_{1-x}\text{Fe}_x\text{O}_2$  using Sol-Gel method. Conductivity studies of lithiated electrolyte materials are important in order to gain a better understanding of the ionic conduction mechanism especially on its usage for lithium ion batteries. Impedance spectroscopy is widely used for investigating the electrical and electrochemical properties. A detailed study on electrical properties of lithiated electrolyte materials as a function of temperature and frequency is necessary to understand the conduction mechanism in  $\text{LiCo}_{1-x}\text{Fe}_x\text{O}_2$  lithiated compound for effective utilization as electrode material in the lithium ion batteries. In the present investigation, the Sol-Gel synthesis of  $\text{LiCo}_{1-x}\text{Fe}_x\text{O}_2$  (with  $x = 0, 0.2, 0.4, 0.7$  and  $1$ ) ceramics, X-ray diffraction studies, SEM & EDS and impedance studies as a function of frequency and temperature were discussed.

### Materials and methods:

$\text{LiCo}_{1-x}\text{Fe}_x\text{O}_2$  ceramics were synthesized using Sol gel method. The starting powders of  $\text{LiNO}_3$  (99.9%),  $\text{Co}(\text{NO}_3)_2 \cdot 6\text{H}_2\text{O}$  (99.9%),  $(\text{FeNO}_3)_3 \cdot 9\text{H}_2\text{O}$  (99.9%) were taken in the stoichiometric ratio and Citric acid ( $\text{C}_6\text{H}_8\text{O}_7$ ) was taken in the 1:2 molar ratio. All the starting materials were dissolved in the distilled water and the  $\text{p}^{\text{H}}$  of the resultant solution was adjusted to 6-7 by adding diluted  $\text{NH}_4(\text{OH})$  solution. Excess lithium was taken to compensate the volatility of lithium. The prepared solution of the starting materials was heated constantly

with continuous stirring. After 48 hours of heating, a thick viscous solution was obtained. To obtain the gel, ethylene glycol was added in the molar ratio 1:1.2. A black porous solid (precursor) was obtained after 5-6 hours of heating at 100°C. The black porous solid was ground and burned in a burner at 300°C to obtain the precursor powder. The precursor was pre-sintered at 800°C temperature for the phase formation. X-ray diffraction studies were carried out on the powder samples of the prepared ceramic powders in the  $2\theta$  range of 10°-80°. After the phase confirmation, the ceramic powders were pressed into circular discs of 1 mm in thick and 10 mm in diameter and these pellets were final sintered at 850°C. Around 90% of the relative densities were obtained for the final sintered samples. Scanning electron microscopy and EDS were taken on the final sintered samples using the ZEISS EVO 18 attached with INCA, Oxford- Energy Dispersive X-ray system. Impedance measurements were carried out for these ceramics in the frequency range 100 Hz – 1 MHz as a function of temperature using AUTOLAB (PGSTAT 30) low frequency impedance analyzer.

**Results and discussion:**

**X-ray diffraction studies:**  $\text{LiCo}_{1-x}\text{Fe}_x\text{O}_2$  (with  $x = 0, 0.2, 0.4, 0.7$  and  $1$ ) well sintered ceramic powders structure is studied by the X-ray diffraction technique carried out in the  $2\theta$  range of 10°-80° and which confirms the single phase for all the samples. The excess of Li avoids the problems associated with lithium volatility and non-stoichiometry and defect interlayer ions in the ceramic oxides.

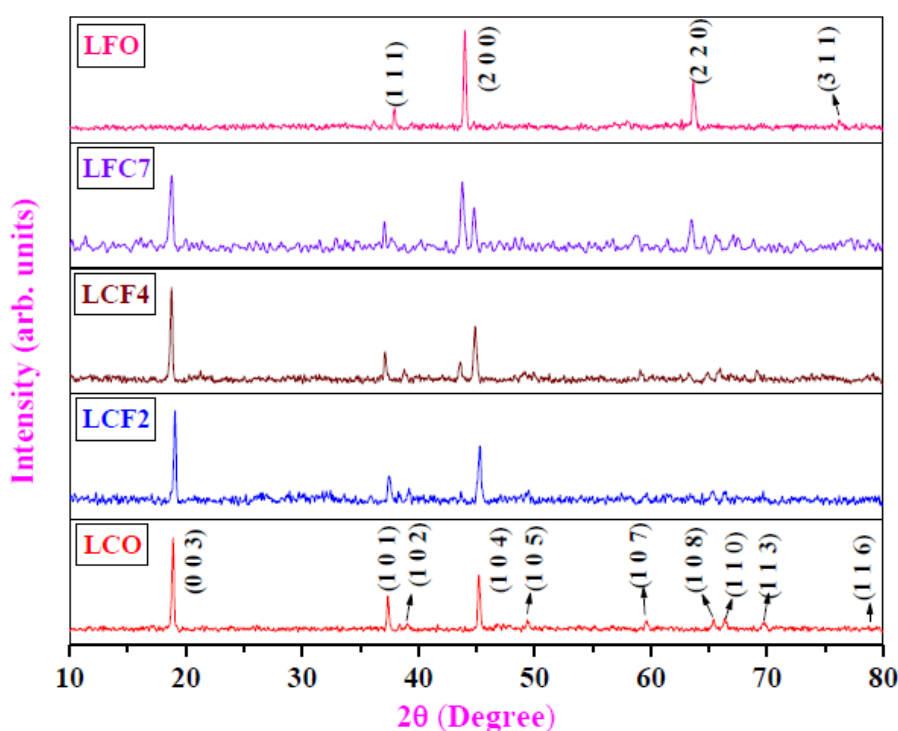


**Figure 1:** Powder XRD patterns of  $\text{LiCo}_{1-x}\text{Fe}_x$  ( $x=0.0, 0.2, 0.4, 0.7$  and  $1.0$ )

Fig 1: shows XRD patterns of compound LCO, LCF2, LCF4, LCF7 and LFO. The position and intensity of LCO and LFO compounds form single phase and the diffraction lines of compound agree with the standard JCPDS card number: 89-7118 for LCO and 82-0340 for LFO with rhombohedral and cubic structures respectively. The unit cell parameters are obtained by least squares fitting and given in Table 1. The XRD spectrum exhibited predominant peak (0 0 3) orientation at  $2\theta = 19.08^\circ$  and also with other characteristic orientations presenting at right positions. The intensity of peak (1 0 4) decreasing, the intensity of peak (2 0 0) increasing and also a merging of (006) and (108) peaks with increasing “Fe” doping concentration in  $\text{LiCoO}_2$  were observed [5]. This indicates a gradual transformation from rhombohedral (R3-m) structure to cubic structure (Fd3m) and an order distribution of lithium ions and transition metal ions exist in the structure. Lattice parameters, experimental density, theoretical density and porosity of the samples were calculated and shown in Table 1.

**Density:** Measurements of densities of material are important, as this measurement gives the information

about the efficiency of atomic packing and the porosity of the materials. The experimental density of the samples was calculated by using the Archimedis principle in xylene media using the relation

$$\rho = \frac{\text{Weight in air of the sample}}{(\text{weight in xylene} - \text{weight in air})} \times (0.865)$$

Where 0.865 is the density of xylene.

The theoretical density (X-ray density) can be calculated using the relation given below (if the number of units of a compound is known).

$$\rho_{th} = \frac{\text{Formula weight (FW)}}{(\text{volume of formula unit} \times N)}$$

N is Avagadro's number, and the relative density also calculated in percentage using formula

$$\rho_r(\%) = (\rho_{exp} / \rho_{th}) * 100$$

Porosity calculated with the experimental density and theoretical density by using formula

$$\text{Porosity}(\%) = (\rho_{th} - \rho_{exp}) / \rho_{th} * 100$$

**Table1:**Lattice parameters,experimental density,theoretical density, relative density and porosity

Compound	M grms	$\rho_{exp}$	Cubic			Rhombhohydral				Porosity (%)
			a(Å)	$\rho_{th}$	$\rho_r$ (%)	a(Å)	c(Å)	$\rho_{th}$	$P_r$ (%)	
LCO	97.660	4.785	-	-	-	2.817	14.013	5.103	93	7
LCF2	97.254	4.981	4.0026	5.036	98	2.817	14.038	5.073	98	2
LCF4	96.637	4.560	4.0393	4.869	93	2.826	14.209	4.948	92	8
LCF7	95.711	4.211	4.0621	4.741	88	2.816	14.222	4.931	85	15
LFO	94.786	3.960	4.169	4.340	92	-	-	-	-	8

Scannig Electron Microscopi (SEM) and EDS:

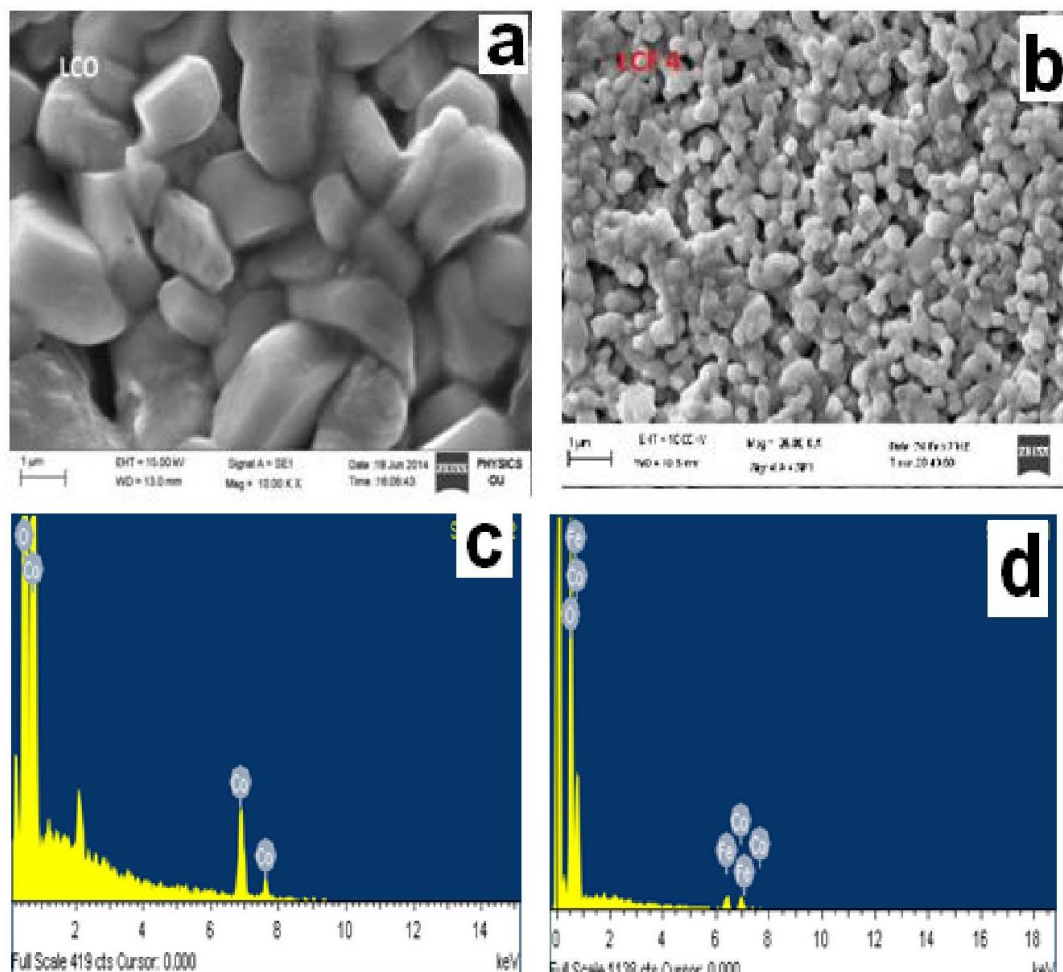


Figure 2(a-d): SEM and EDS images of samples LCO and LCF4

The morphology and micro structural studies of LCO and LCF4 compounds were obtained from the Scanning electron microscope (ZEISS EVO<sup>®</sup> series SEM), the scanning electron micrograph and EDS spectra of the sintered samples of LCO and LCF4 images are shown in Figure 2a and 2b. These micrographs indicates that the samples consist of homogeneously distributed spherical and cylindrical shaped grains present in the samples are dense with the grain size of 1 $\mu$ m [3].

In order to investigate the chemical composition of samples, the Energy-dispersive X-ray spectroscopy (EDS) analysis with a beam controller was done on the surface of the pellets. Figure 2c and 2d showing EDS of LCO and LCF4 samples. EDS spectra indicate the existence of Fe, Co and O<sub>2</sub> in the desired proportion. Li has very low energy of characteristic radiation, its binding energy cannot be possible to detect from EDS data [6]. No other impurity peaks are detected in the spectrum, which is an indication of the chemical purity of the sample

**Impedance analysis:** The impedance spectroscopy measurements was done for all samples with PGSTAT30 AUTO LAB. The graph is plotted with real part of impedance ( $Z'$ ) and imaginary part of impedance ( $Z''$ ) at different temperatures with varying frequencies, which shows the partial cole-cole plots indicates the not originated from the center of the axis within done frequency range (100Hz -1MHz) shown in Fig3(a) because of the sample LCF2 having high conductivity may obtain complete cole-cole plots at higher frequencies.

And for the sample LCF4 cole-cole plots were observed with different temperatures and the center of semicircle lies below real axis Fig 3 (b) which indicates the Non Debye nature. This sample have greater magnitude of resistance value because with increasing Fe concentration in host compound, this resistivity nature suddenly falls to lower value with increasing temperature due to ionic hopping. The LFO compound shows high resistivity and Non Debye type cole-cole plots shown in Fig.3 (c), the fitted parameters were calculated and shown in Table 2.

Inset figure shows the fitted data LFO, LCF2 and LCF4 which is fitted using Z-view software and fitted parameters also calculated is shown in Table 2. The semicircles are subjected to nonlinear least square fitting. The equivalent circuit used for this purpose is shown in Fig 6 are explained as follows: the element Rs represent the series resistance or balance resistance. As the two capacitive semicircles are depressed, a constant phase element (CPE) is taken in the place of

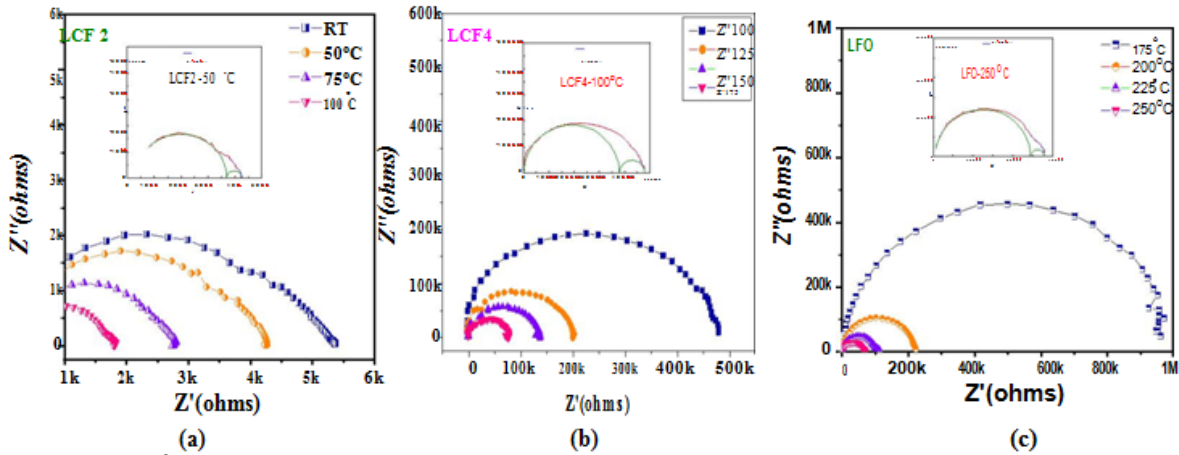


Figure 3(a-c): Cole-Cole plots and fitting parameters (inset figures) of (a) LCF2, (b) LCF4 and (c) LFO

capacitance at high frequency region semicircle  $R_g$  and  $CPE_g$  represent due to grain and at low frequency region semicircle  $R_{gb}$  and  $CPE_{gb}$  due to grain boundary. The CPE arises due to microscopic materials properties. The interfaces between the electrode are not smooth and uniform, as the electrodes are made using fine particles of the active materials [5, 6]. Reaction resistance and capacitance may differ with the electrode position. The admittance representation of CPE is given as

$$Y^* = A_0 (j\omega)^n \quad (0 < n < 1)$$

Where  $A_0$  is adjustable parameter and  $\omega = 2\pi f$ ,  $f$  is AC frequency. For  $n=0$ , CPE acts as resistance  $R (=A_0^{-1})$ ; for  $n=1$ , a capacitance  $C (=A_0)$ . Fig 4 represents the conductivity plot which is drawn between frequency, ac conductivity for samples LCF2, LCF4 and LFO respectively. The figure clearly indicates the slightly frequency dependent nature of the samples LCF2, LCF4 and which having almost frequency independent curves, sample LFO having two clearly distinct regions one is rapid frequency dependent region other is plateau like frequency independent region.

Figures 5 show Arrhenius plots of LCF1, LCF2 and LFO compounds and also clearly reveal the increasing of conductivity with increasing temperature. The activation energy is calculated with below formula.

$$\sigma = \sigma_0 \exp(-E/kT)$$

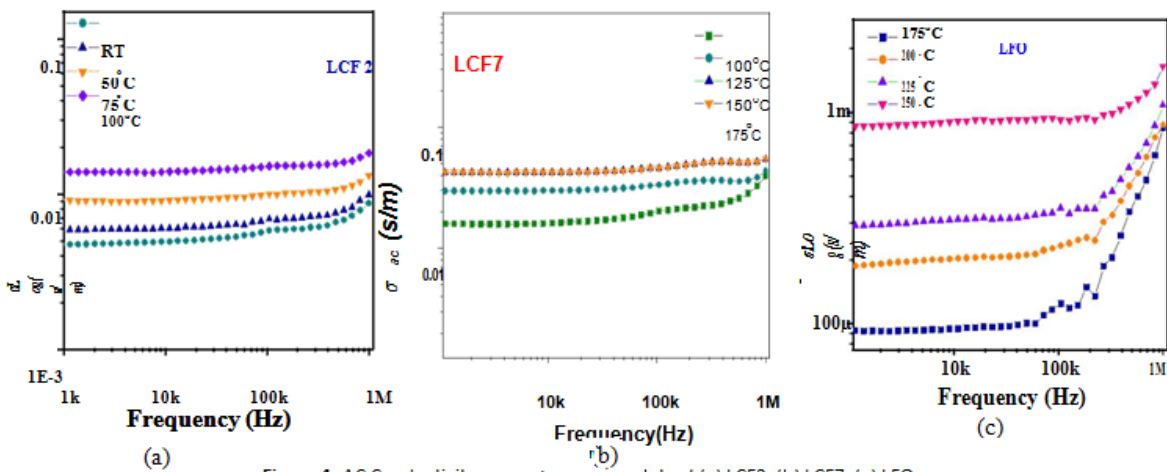


Figure 4: AC Conductivity versus frequency plots of (a) LCF2, (b) LCF7, (c) LFO.

The activation energy of the sample was calculated from the slope of the plots drawn between the  $1000/T$  and  $\text{Log}\sigma$  linear fitted lines shown in Fig.5. The activation energy of the samples for LCF1 is 0.43 eV, LCF2 is 0.17 eV, LFO is 0.09 eV. From this one can know the decreasing in activation energy with increase doping ferrous concentration in  $\text{LiCo}_{1-x}\text{Fe}_x\text{O}_2$  compound and also increases of conductivity.

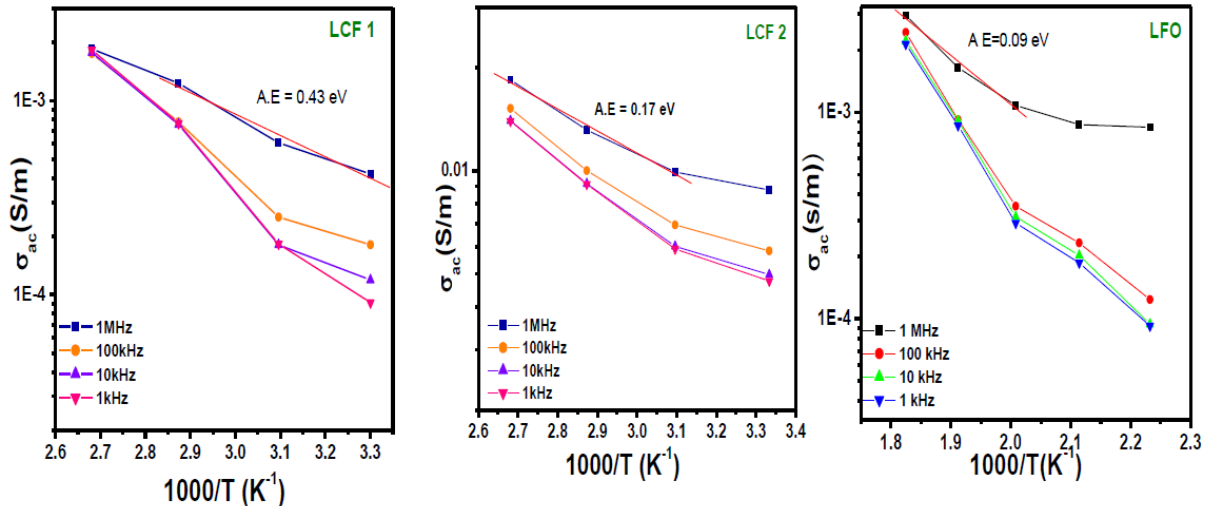


Figure 5: AC conductivity versus absolute temperature plots of LCF1, LCF2, LFO.

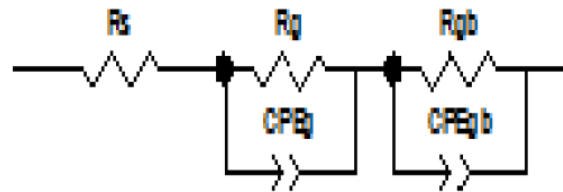


Figure 6: Appropriate equivalent circuit with fitting parameters

Table 2: Fitting parameters of LFO, LCF2 and LCF4 at different temperatures

Compound	T (°C)	$R_s$ (Ω)	$R_g$ (Ω)	CPE <sub>g</sub>		$R_{gb}$ (Ω)	CPE <sub>gb</sub>	
				$A_0$	$n$		$A_0$	$n$
LFO	175	3744	974890	$6.52 \times 10^{-10}$	0.96	---	---	---
	200	1882	215790	$3.38 \times 10^{-10}$	0.98	---	---	---
	225	1260	12281	$3.35 \times 10^{-7}$	0.96	99458	$4.616 \times 10^{-11}$	0.96
	250	1310	10000	$9.98 \times 10^{-7}$	0.96	59800	$6.93 \times 10^{-8}$	0.99
LCF2	RT	272	859	$1.21 \times 10^{-6}$	0.99	4140	$1.38 \times 10^{-10}$	0.98
	50	302	571	$4.41 \times 10^{-6}$	0.99	3397	$1.17 \times 10^{-10}$	0.99
	75	252	299	$1.11 \times 10^{-6}$	0.99	2261	$1.17 \times 10^{-10}$	0.99
	100	222	175	$1.11 \times 10^{-5}$	0.99	1451	$1.27 \times 10^{-10}$	0.99
LCF4	100	340	99810	$3.10 \times 10^{-6}$	0.99	379440	$5.15 \times 10^{-11}$	0.98
	125	340	32810	$2.20 \times 10^{-6}$	0.99	167440	$4.25 \times 10^{-11}$	0.96
	150	340	21210	$1.10 \times 10^{-6}$	0.99	115850	$3.25 \times 10^{-11}$	0.95
	175	340	8210	$4.10 \times 10^{-6}$	0.99	68960	$4.55 \times 10^{-11}$	0.96

Conclusions:

$\text{LiCo}_{1-x}\text{Fe}_x\text{O}_2$  compound was prepared by sol-gel method. Phase formation of the samples studied from X-Ray diffraction technique which confirms the rhombohedral and cubic structure. Surface morphology of the samples were studied by Scanning electron microscopy particle size was estimated to be about  $1\mu\text{m}$ . The impedance data shows Non-Debye nature and different relaxation times present in the samples at different temperatures. Resistance and capacitance of the grain and grain boundary values were calculated by fitting an appropriate equivalent circuit to the Cole-Cole plots. Frequency dependent conductivity follows the universal power law. Temperature dependent conductivity follows the Arrhenius law and calculated activation energies which are decreased (0.43eV for LCF1, 0.17eV for LCF2 and 0.09eV for LFO) with increased “Fe” doping.

**Acknowledgements:**

The authors thank the UGC-UPE-FAR program of Osmania University for financial assistance.

**REFERENCES**

- [1] Chapel .E , Holzapfel. M, Chouteau. G, et. al, Effect of cobalt on the magnetic properties of the  $\text{LiCo}_{1-x}\text{Co}_x$  layered system ( $0 \leq x \leq 1$ ). J Solid State Chem, 2000, 154:451-459.
- [2] Alcantara. R, Lavela. P, Perez Vicente. C, et.al, X-ray and neutron diffraction, Fe Mossbauer spectroscopy and X-ray absorption spectroscopy studies of iron substituted lithium cobaltate. Solid State Commun, 2000, 115:1-6.
- [3] Wenbin Lue, Xinhai Li, and Dahn. J.R, Synthesis and Charecterization of Mg substituted  $\text{LiCoO}_2$ . J Electrochem Soc.2010, 157(7):A782-A790.
- [4] Suresh P, Shukla A. K, Munichandraiah. N, Synthesis and characterization of  $\text{LiFeO}_2$  and  $\text{LiFe}_{0.9}\text{Co}_{0.1}\text{O}_2$  as cathode materials for Li-ion cells. J Power Sources, 2006, 159:1395-1400.
- [5] Suresh. P, Rodrigues S, Shukla A. K,et.al Synthesis of  $\text{LiCo}_{1-x}\text{Mn}_x\text{O}_2$  from a low temperature route and characterization as cathode materials in Li-ion cells. Solid State Ionics, 2005, 176:281-290.
- [6] Rosaiah P, Hussain O. M, Synthesis, electrical and dielectrical properties of lithium iron Oxide. Adv. Mat. Lett,2013, 4(4):288-295.